Psychophysiology, 47 (2010), 133–146. Wiley Periodicals, Inc. Printed in the USA.

DOI: 10.1111/j.1469-8986.2009.00880.x

Novelty P3 reductions in depression: Characterization using principal components analysis (PCA) of current source density (CSD) waveforms

CRAIG E. TENKE,[a,b] JÜRGEN KAYSER,[a,b] JONATHAN W. STEWART,[b,c] AND GERARD E. BRUDER[a,b]

[a]Division of Cognitive Neuroscience, New York State Psychiatric Institute, New York, New York, USA
[b]Department of Psychiatry, Columbia University College of Physicians and Surgeons, New York, New York, USA
[c]Depression Evaluation Service, New York State Psychiatric Institute, New York, New York, USA

Abstract

We previously reported a novelty P3 reduction in depressed patients compared to healthy controls ($n = 20$ per group) in a novelty oddball task using a 31-channel montage. In an independent replication and extension using a 67-channel montage ($n = 49$ per group), reference-free current source density (CSD) waveforms were simplified and quantified by a temporal, covariance-based principal components analysis (PCA) (unrestricted Varimax rotation), yielding factor solutions consistent with other oddball tasks. A factor with a loadings peak at 343 ms summarized the target P3b source as well as a secondary midline frontocentral source for novels and targets. An earlier novelty vertex source (NVS) at 241 ms was present for novels, but not targets, and was reduced in patients. Compatible CSD-PCA findings were also confirmed for the original low-density sample. Results are consistent with a reduced novelty response in clinical depression, involving the early phase of the frontocentral novelty P3.

Descriptors: Event-related potential (ERP), Principal components analysis (PCA), Current source density (CSD), Surface Laplacian, Oddball task, P300, Depression, Novelty P3

The archetype of cognitive event-related potential (ERP) components is a positivity that can be recorded at around 300 ms poststimulus (P300 or P3; Sutton, Braren, Zubin, & John, 1965), which has been identified in diverse paradigms. However, it soon became clear that the apparent ubiquity of P3 obscured an underlying distinction between separable subcomponents of a late positive complex (Squires, Squires, & Hillyard, 1975; Sutton & Ruchkin, 1984), and that quantification strategies suited to simple sensory-evoked potentials (i.e., reference-dependent peak or window measures) were inadequate for components with broad, overlapping time courses and topographies (Donchin, 1966; Glaser & Ruchkin, 1976; Kayser & Tenke, 2005). The de facto standard task for studying target-related P3 (P3b) is the two-stimulus oddball task, consisting of frequent standard stimuli and infrequent targets. We recently exploited the familiarity of this well-known ERP paradigm with auditory stimuli to evaluate a generic new approach to the identification and measurement of ERP components. This methodology relies on refinements of well-established techniques, current source density (CSD) and principal components analysis (PCA), to separate components having simpler topographies that are unaffected by the recording reference and that are more closely related to the underlying neuronal generators (Kayser & Tenke, 2006b; Tenke et al., 2008). Apprehensions about the attenuation of components arising from deep or distributed generators by the CSD transformation (e.g., Nunez & Srinivasan, 2006) were not supported for group comparisons (Kayser & Tenke, 2006b). CSD-PCA solutions were surprisingly stable, resulting in comparable component structures for the same binaural oddball tasks using low-density (31-channel) and high-density (129-channel) montages (Kayser & Tenke, 2006c) as well as for a unique oddball task using dichotic stimuli (Tenke et al., 2008). In our implementation of the oddball task, the P3 source factor for targets had a characteristic parietotemporal topography.

This work was supported in part by Grants MH36295 and MH66597 from the National Institute of Mental Health. The authors are grateful for the assistance of Christopher J. Kroppmann, Nathan A. Gates, and Jennifer D. Schaller in collecting and processing the data. We also acknowledge the waveform plotting software written by Charles L. Brown, III. Finally, we appreciate the suggestions of two anonymous reviewers, which greatly improved this article.

Address reprint requests to: Jürgen Kayser, New York State Psychiatric Institute, Division of Cognitive Neuroscience, Unit 50, 1051 Riverside Drive, New York, NY 10032, USA. E-mail: kayserj@pi.cpmc.columbia.edu

P3 Source Topographies in the Novelty Oddball Task

Courchesne, Hillyard, and Galambos (1975) introduced a new class of infrequent, unexpected, and task-irrelevant stimuli into a visual oddball task (recognizable geometric shapes and novel, unfamiliar patterns). Although targets and irrelevant shapes both resulted in a posterior P3, novel stimuli produced a prominent, early frontal P3, preceded by a large N2. Within the context of an auditory oddball task, an increase in the salience of a class of stimuli (e.g., incidence probability or uniqueness) also elicits an early (233–278 ms), fronto-

central positivity (P3a), even if the stimuli are ignored (Squires et al., 1975). Knight (1984) used a variation in which an irrelevant novel sound (a dog bark) was presented, and observed and enhanced, shorter-latency N2 (Cz maximum), followed by a frontocentral P3 that decreased over the first five presentations. Patients with frontal lesions showed neither the enhanced N2 nor the frontocentral P3.

The auditory novelty oddball task now generally includes a class of trial-unique, novel stimuli (animal sounds, musical instruments, environmental sounds), which in turn elicit an early, anterior novelty P3 (Friedman, Simpson, & Hamberger, 1993). Considerable effort has been applied in determining the functional and topographic (and by implication, neuronal generator) properties of this novelty P3, and a strong case has been made for its identification as P3a (Friedman, Cycowicz, & Gaeta, 2001; Polich, 2007; Simons, Graham, Miles, & Chen, 2001; Spencer, Dien, & Donchin, 2001). The idea that novelty P3/P3a reflects frontal attentional processes related to the orienting response (Friedman, Cycowicz, & Gaeta, 2001; Polich, 2007) is also consistent with evidence that novelty P3 (but not P3b following novelty P3) is associated with the electrodermal orienting response (Marinkovic, Halgren, & Maltzman, 2001).

Based on the topographic and temporal distinction between the novelty P3 and target P3b in the same task, spatial PCA methods have confirmed the characteristic midline frontocentral topography of novelty P3 (Spencer et al., 2001), as does cortical image transformation (deblurring; He, Lian, Spencer, Dien, & Donchin 2001) and the related, but simpler, surface Laplacian (Friedman et al., 2001). When probed using intracranial electrodes (oddball task; nose reference), P3a typically appears as part of the triphasic component sequence, N2a/P3a/SW (Halgren et al., 1995). In the vicinity of the posterior cingulate gyrus, the potential gradients are steep, suggestive of proximity to a generator. However, the same component sequence is seen within the frontal lobe as well (Baudena, Halgren, Heit, & Clarke, 1995), but with no significant differences between distracters and targets, and is characterized by steep intracranial field potential gradients near the inferior frontal sulcus. Findings more consistent with the scalp topography of the novelty P3 are the large amplitudes (>100 μV) and steep gradients in orbitofrontal regions, with polarity inversions at the most medial sites. In a summary of their recordings, Halgren, Marinkovic, and Chauvel (1998) noted "clear inversions of the P3a occurred in the anterior cingulate cortex and its inferior extension, the gyrus rectus" (p. 160) thereby directly implicating these regions as possible generators of the novelty P3.

Volume Conduction and Source Localization: Putative Midline Generators of Novelty P3

CSD analysis is the simplest of a number of generator localization approaches based on the volume conduction model, which may be expressed as a vector form of Ohms law:

$$\mathbf{J} = \sigma\mathbf{E} \tag{1}$$

where **J** is current flow density, **E** is the electric field (i.e., gradient of the measured field potential) and **σ** is the conductivity tensor of the medium. The most concrete application of Equation (1) is a direct simplification in the form of Poisson's source equation, which allows the quantification of current generators (sources and sinks) in intracranial (CSD laminar profile of cortical regions) or scalp data (surface Laplacian; radial scalp current density[1]). This relationship applies equally to measured and inferred intracranial fields, and thereby provides a common, multiresolutional framework into which findings from scalp ERPs, inverse models (e.g., brain electrical source analysis (BETA), low resolution brain electromagnetic tomography (LORETA)), and intracranial studies may be integrated (Tenke & Kayser, 2005).

Dien, Spencer, and Donchin (2003) used a dipole inverse model to support the anterior cingulate cortex (ACC) as a generator of novelty P3. An ACC solution has since been replicated (Debener, Makeig, Delorme, & Engel, 2005), even when the location of the dipole inverse solution has been constrained based on fMRI (Crottaz-Herbette & Menon, 2006). However, ERP and fMRI measures differ considerably both in their temporal and spatial resolution and in their biophysical substrates, suggesting that this convergence is quite fortuitous. Moreover, as previously argued (Kayser & Tenke, 2006b; Tenke & Kayser, 2005), cortical generators should be characterized by local current flow approximately normal to the cortical surface (i.e., aligned with projection cells; Klee & Rall, 1977; Lorente de No, 1947; Tenke, Schroeder, Arezzo, & Vaughan, 1993). What at first glance appears to be a parsimonious convergence of findings across methodologies actually introduces an electrophysiological paradox: Unless the generator is restricted to the banks of the cingulate sulcus, rather than the cingulate gyrus itself, the equivalent dipole should be tangential to the midline scalp. In this regard, it is notable that a tangential generator is consistent with published CSD maps of novelty P3, in which a midline source may be coupled with lateral sinks (cf. Figures 5 and 8 of Friedman et al., 2001).

Misgivings about the anatomical or physiological adequacy of inverse solutions have led some seasoned investigators to question ERP generators localized by inverse models to the cingulate gyrus. Given the possible commonality of P3a and the no-go P3 produced in go/no-go tasks (Polich, 2007), it is of interest that when Verleger, Paehge, Kolev, Yordanova, and Jaskowski (2006) localized an equivalent dipole for go/no-go P3 to midline cingulate cortex between areas 24 and 23 (i.e., near motor areas), the authors acknowledged the possibility ". . .that this is simply the center-of-mass of some widespread effect. . . ." (p. 311). Likewise, Mathalon, Whitfield, and Ford (2003) recognized the possibility of misallocation by a single midline dipole solution for error-related negativity (ERN) in the anterior cingulate. We defer this discussion to another paper (Tenke & Kayser, 2008), noting only that the apparent precision with which neuronal generators have been localized may be illusory. The precise regional and laminar generator patterns underlying the novelty P3 are still poorly understood.

None of the above considerations affect the validity of the surface Laplacian or CSD. To the contrary, they underscore the consistency of these methods, and suggest that the efficient descriptions provided by CSD-PCA may, at times, be more relevant to the generator localization problem than a precise, but model-dependent, inverse solution that leads to erroneous conclusions. Being immune to the nonuniqueness that plagues inverse models (i.e., multiple solutions using a different number of generators are equally valid), or by their assumptions about the nature and distribution of underlying neuronal generators (i.e., number and orientation of dipoles; orientation of intracranial current flow), scalp-based CSD recordings provide a conservative description of the source image at the scalp, while also imposing constraints by which the physiological plausibility of a generator may be evaluated.

[1]Although previously assumed, the compatibility of surface Laplacian measures with the radial transcranial currents of a volume model has been verified by Yao (2002), thereby providing the necessary bridge between surface measures and the underlying model implied by Equation (1).

Novelty P3 in Depressed Patients

P3 reductions in depression have been reported using a challenging dichotic listening test (Bruder et al., 1995), and a dichotic oddball task (Tenke et al., 2008). However, reports of reductions in simpler oddball tasks have been inconsistent (for reviews, see Bruder, Kayser, & Tenke, in press Roth, Duncan, Pfefferbaum, & Timsit-Berthier, 1986), and may be dependent on patients' clinical characteristics. In a binaural oddball task, Bruder et al. (2002) reported an early P3 factor (nose reference; 315 ms peak latency), having a topography that included midline frontocentral sites, which was separable from a later P3 (400 ms) subcomponent, with a parietal topography typical of P3b. The former factor was larger in patients having an anxiety disorder alone when compared to depressed patients or healthy controls. Patients having depressive disorder with comorbid anxiety disorder, but not depression alone, tended to have a smaller early P3 than healthy controls. In contrast, the late P3 was larger in depressed patients having a comorbid anxiety disorder when compared to the other groups, but did not differ between patients having a depressive disorder alone and controls. If P3a is as ubiquitous as suggested by Polich (2007), the early P3 differences could reflect P3a differences between groups.

The importance of differentiating between P3 subcomponents is that they are associated with different cognitive operations and neural generators (Polich, 2007), and this could provide new information on the cognitive and neural correlates of P3 reductions in depressed patients. Although novelty P3 is generally considered to be a variant of P3a, it is paradigmatically and functionally distinct from target-related P3b. In a preliminary report using integrated window amplitudes as component measures for 31-channel, nose-referenced ERPs recorded during a binaural novelty oddball task, we observed a prominent reduction in an early, frontocentral novelty P3 for 20 depressed patients when compared to 20 healthy controls (Bruder, Kroppmann, et al., 2009; Kroppmann et al., 2006). However, reliance on conventional ERP measures posed limitations for a complete separation of novelty P3 from overlapping late positive components. The present study sought to replicate and extend these findings in an independent and substantially larger sample ($N = 98$; 49 depressed patients) using a denser 67-channel recording montage so as to identify and quantify the underlying scalp current generator patterns derived from reference-free CSD-PCA methodology. Findings were compared with analogous CSD-PCA solutions obtained from the previous, smaller sample ($N = 40$) using a 31-channel montage, and interpreted in the context of solutions obtained for other auditory oddball tasks.

Methods

Participants

Healthy adults ($n = 49$; 23 male) with no history of psychopathology, and depressed outpatients ($n = 49$; 22 male) from the Depression Evaluation Service at the New York State Psychiatric Institute were recruited from the New York metropolitan area. Table 1 shows the demographic characteristics of the sample. Participants were excluded from the study if they had a hearing loss greater than 30 dB in either ear at 500, 1000, or 2000 Hz, or if they had an ear difference greater than 10 dB. Participants were also excluded if they had current substance abuse, a history of head trauma, or other neurological disorder. Patients were all drug free for a period of at least 7 days. Control participants were screened using the Structured Clinical Interview for *DSM-IV*, nonpatient edition (First, Spitzer, Gibbon, & Williams, 1996) to exclude those with current or past psychopathology. Participants in both groups were predominantly right-handed as indicated by their Laterality Quotient (LQ) using the Edinburgh Inventory (Oldfield, 1971). Although handedness has been reported to influence the amplitude of anterior P3 (Alexander & Polich, 1995), four left-handed patients ($LQ < 0$) were included because critical findings were preserved when these patients were excluded. Reports of nicotine use, which may affect P3 amplitude (Anokhin et al., 2000), were not solicited. Most patients met *DSM-IV* criteria for major depressive disorder (MDD; $n = 26$), dysthymia ($n = 9$), or both disorders ($n = 11$). Of the remaining 3 patients, 1 was bipolar (depressive phase) and 2 had diagnoses of depression not otherwise specified. Eight patients had a comorbid anxiety disorder. Beck Depression Inventory (Beck, Ward, Mendelson, & Erbaugh, 1961) scores of patients ranged from 13 to 41 (mean = 23.0 ± 7.2).

Table 1. *Demographic Variables*

	Patients (n = 49; 22 male)		Healthy controls ($n = 49$; 23 male)	
Variable	Mean	*SD*	Mean	*SD*
Age (years)[a]	35.8	10.7	31.0	10.6
Education (years)	15.5	2.5	15.7	2.6
BDI	23.0[b]	7.2	1.7[c]	2.5
Ethnicity				
Caucasian	32		32	
Black	3		5	
Asian	2		2	
Native American	1		0	
Multiracial	9		5	
Unknown	2		5	

[a]Significant group difference: $t = 2.24$, $df = 96$, $p = .03$.
[b]$n = 48$.
[c]$n = 46$.

Novelty Oddball Task

An auditory novelty oddball task was implemented on a Neuroscan STIM system using stimuli developed for this task (Friedman et al., 1993). For each subject, eight blocks of 50 trials consisting of two 300-ms tones were presented in pseudorandom order (1000 ms stimulus onset asynchrony; 10 ms rise and fall time). A nontarget tone of 350 Hz was presented to the subjects frequently ($p = .76$), as well as an infrequent target tone ($p = .12$) of 500 Hz. Novel sounds (i.e., animal sounds, musical instruments, environmental sounds) with durations of 100–400 ms were infrequently ($p = .12$) intermixed with the nontarget and target tones. All stimuli were presented binaurally over headphones at 85 dB SPL. Subjects were instructed to focus their eyes on a fixation cross displayed on a computer monitor, and to respond with a button press as quickly as possible when, and only when, they heard the infrequent target tone. Response hand (right or left) was counterbalanced across blocks, and will not be considered further in this report.

ERP Methods

Subject preparation. A Lycra stretch electrode cap was used to record from a 66-channel, expanded 10–20 scalp montage (Pivik et al., 1993), with additional channels for nose (used as off-line reference) and bipolar eye activity (left [LE] and right [RE] outer canthi; above [TE] and below [BE] right eye) to monitor lateral eye movements and blinks. Cap placement was optimized by precise

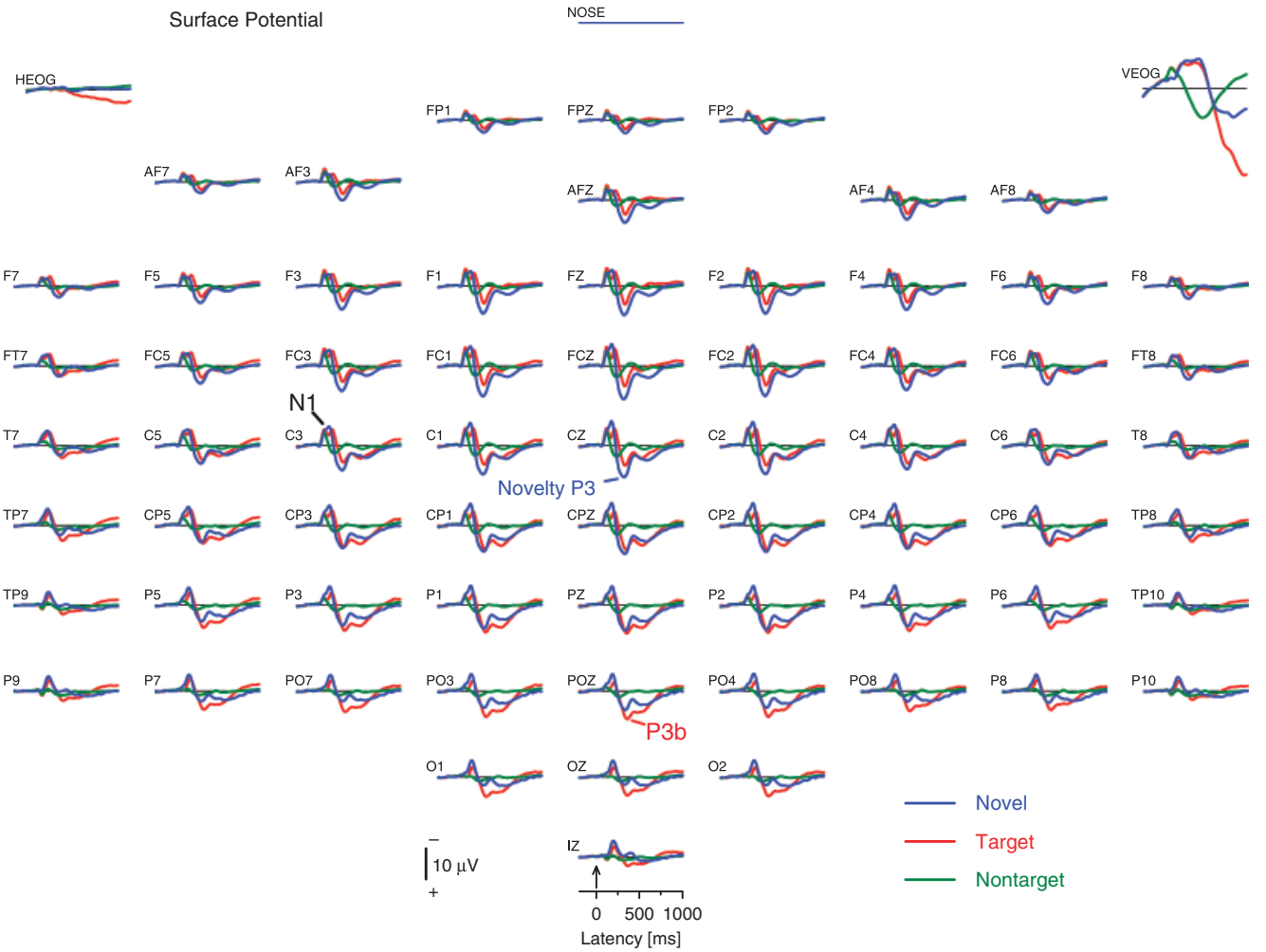

Figure 1. Grand average nose-referenced surface potential (ERP) waveforms for correct targets, nontargets, and novels at all 67 recording sites. Components N1, target-P3b, and novelty P3 are indicated at sites C3, POz, and Cz.

measurements of electrode locations with respect to landmarks of the 10–20 system (nasion, inion, auditory meatus, vertex). The scalp placements were prepared using a conventional water soluble electrolyte gel, and the electrode–scalp interface was verified by the acquisition software (ActiView; BioSemi, 2001). During acquisition, the active recording reference was composed of sites PO1 (common mode sense) and PO2 (driven right leg).

Recording and preliminary processing. Continuous electroencephalogram (EEG), stimulus onset, and response codes were recorded using a 72-channel, 24-bit Biosemi ActiveTwo system (256 samples/s; DC-128 Hz). After acquisition, raw data were converted to a nose reference, bipolar EOG derivations were computed from the four eye channels (horizontal electrooculgram (HEOG) = RE – LE; vertical electrooculogram (VEOG) = TE – BE) and exported to 16-bit Neuroscan format using Polyrex (Kayser, 2003), a widely used conversion program that removes ActiveTwo DC offsets, optimizes data rescaling for 16-bit resolution, and provides EEG re-referencing. Amplifier drift was eliminated by padding sufficient samples into the beginning of the file and applying a high-pass causal filter based a rectangular smoothing window (3541-point padding/channel allows the buildup of a rectangular filter window, corresponding to a 10-s time constant[2]). The filtered, continuous EEG was then blink corrected using a spatial, singular value decomposition filter generated from identified blinks and artifact-free EEG periods (NeuroScan, 2003).

Stimulus-locked epochs (1200 ms, 200 ms prestimulus) were extracted. ERP waveforms were screened for electrolyte bridges (Tenke & Kayser, 2001). Channels containing amplifier drift, residual eye activity, muscle or movement-related artifacts, or noise for any given trial were identified using a reference-free approach (Kayser & Tenke, 2006a), and replaced by spherical spline interpolations (Perrin, Pernier, Bertrand, & Echallier, 1989) using the data from artifact-free channels if possible (i.e., when less than 25% of all EEG channels contained an artifact), as verified by visual inspection. ERP averages were computed for correct targets, nontargets, and novels (at least 16 trials for all averages), as well as for novels in the first and last halves of blocks (valid data containing at least 8 trials was available for 47 controls and 44 patients). ERP averages were then low-pass filtered at 12.5 Hz (– 24 dB/octave) and finally baseline corrected using the 200 ms preceding stimulus onset. Visual inspection of the individual ERP waveforms confirmed a satisfactory signal-to-noise ratio for each participant and each condition.

[2]Highpass cutoff frequency based on rectangular smoothing window is 0.0159 [Hz] = .44 ∗ (256 [samples/s])/(2 ∗ 3541 [sample points]+1).

Figure 1 shows grand average, nose-referenced ERP averages for correct trials in the novelty oddball task. The expected component structure was observed, including novelty P3 (indicated at vertex, electrode Cz) and a posterior target P3b.

CSD methods

Current source density. CSD estimates are based on the second spatial derivative of the recorded surface potentials and represent the magnitude of the radial (transcranial) current flow entering (sinks) and leaving (sources) the scalp (Nunez & Srinivasan, 2006). CSD is a true reference-free technique, in that any ERP recording reference scheme will provide identical CSD estimates, which resolves the ubiquitous problem of arbitrarily choosing a reference. Moreover, by eliminating volume-conducted contributions from distant regions, CSD topographies have more sharply localized peaks than corresponding ERP topographies, and more closely represent the direction, location, and intensity of current generators that underlie an ERP topography (Mitzdorf, 1985; Nicholson, 1973). Furthermore, CSD waveforms have more focal temporal peaks than the corresponding ERP waveforms (Kayser & Tenke, 2006b), thereby providing a more precise time course of any given ERP/CSD component. Although CSD estimates are montage dependent, the surprising accuracy and reliability of low-density estimates support the comparability of high- and low-density CSD solutions, particularly for group comparisons (Kayser & Tenke, 2006c).

Figure 2 shows CSD grand averages for correct trials. CSD estimates ($\mu V/cm^2$ units; 10-cm head radius) were computed using a spherical spline surface Laplacian (Perrin et al., 1989) with computation parameters (50 iterations; $m = 4$; smoothing constant $\lambda = 10^{-5}$) previously established for a 31-channel recording montage (e.g., Kayser & Tenke, 2006b, 2006c; Tenke et al., 1998). As expected, components have sharper topographies and time courses that more clearly separate the anterior from posterior P3 sources.

CSD-PCA. As detailed in Kayser and Tenke (2006b), event-related CSDs were submitted to a covariance-based PCA followed by unrestricted Varimax rotation of the covariance loadings (Matlab emulation of BMDP-4M published in the appendix of Kayser & Tenke, 2003). Data consisted of 308 time points as variables (– 200 to 1000 ms), using a total of 19,698 observations as cases consisting of three conditions (novel, target, nontarget), 98 participants, and 67 sites (electrode locations).

Figure 3 shows the obtained CSD-PCA factor structure for the novelty oddball task, and Table 2 indicates its comparability with that observed in other oddball tasks using two-stimulus binaural (Kayser & Tenke, 2006b, 2006c) and dichotic (Tenke

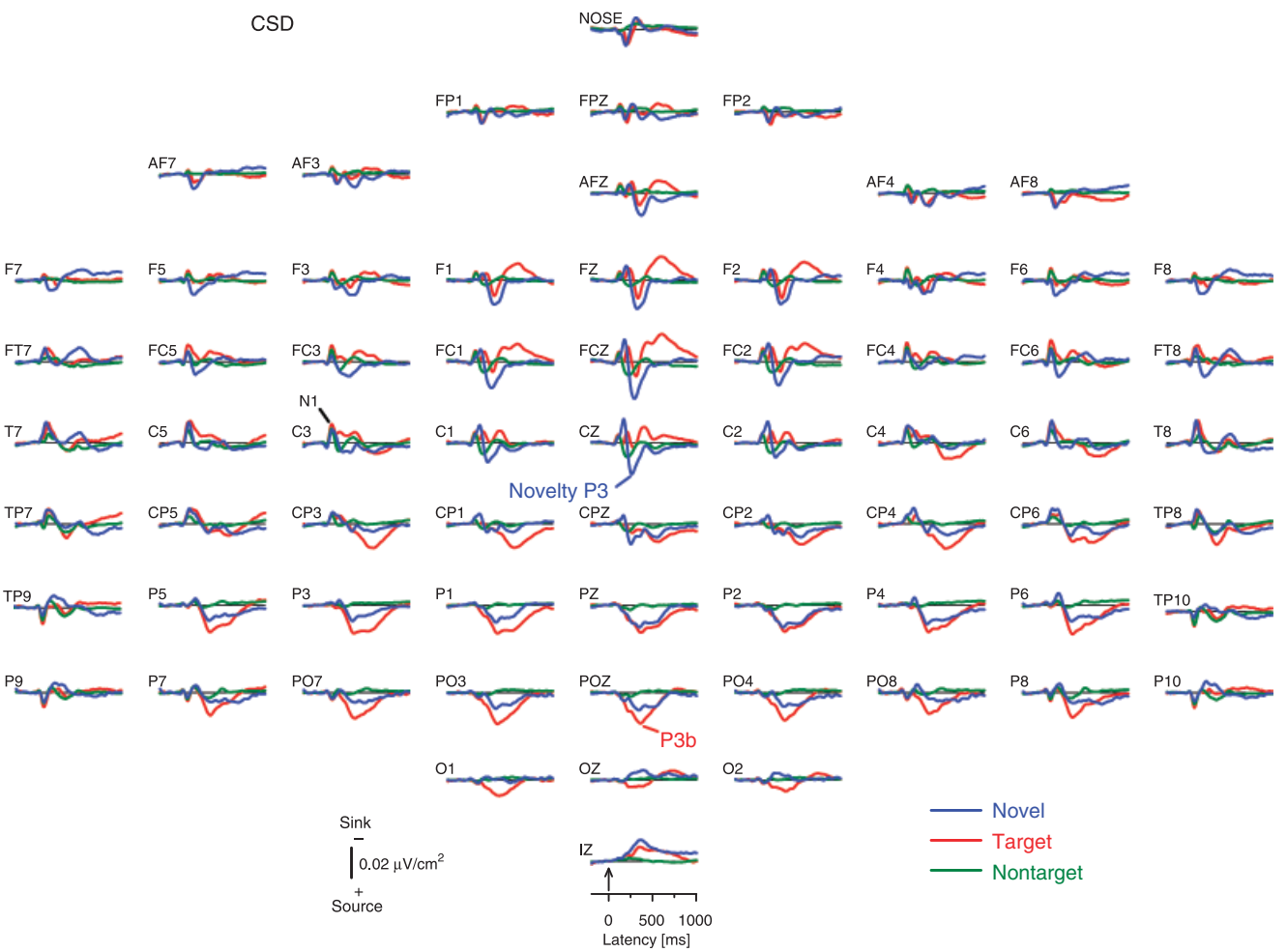

Figure 2. Surface Laplacian (CSD) waveforms corresponding to the ERPs shown in Figure 1. Components N1 sink, target-P3b source, and novelty P3 source are indicated at sites C3, POz, and Cz. Scale: negative-up (sink).

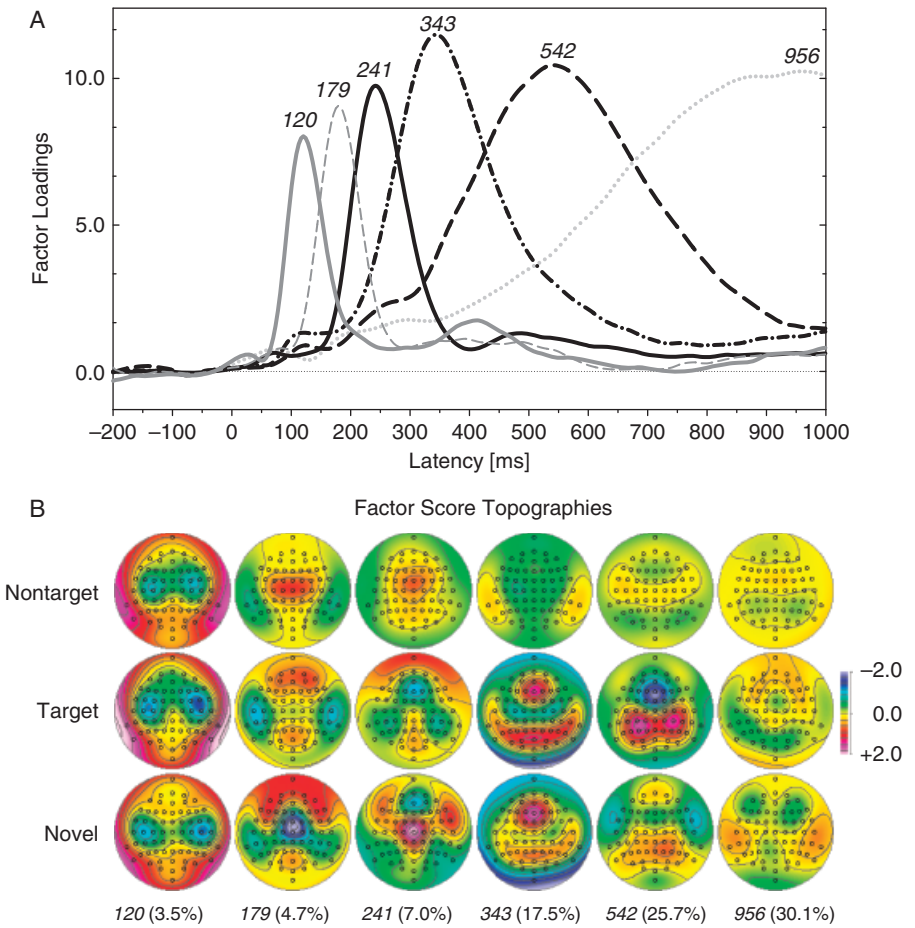

Figure 3. A: Unrestricted temporal PCA solution for CSD waveforms. Factor loadings waveforms of first six factor extracted (by variance). Labels indicate factor loadings peak latency. B: Corresponding average factor score topographies of first six factors for correct nontargets, targets, and novels. Factors are identified by peak latency and percent of variance accounted for (in parentheses). Scale: blue sink, red source.

et al., 2008) stimuli. Factors representing N1, temporal N1, N2, P3, and a late positivity (F – CP+) were readily identifiable from loadings waveforms and corresponding factor score topographies. Specifically, an N1 (*120*) sink/source topography was observed that was similar in all stimuli, and consistent with activation of primary auditory cortex within the Sylvian fissure (tangential N1; sink maxima near sites C3/C4; Figure 3b). A subsequent sink (temporal N1; *179*; Figure 3b, column 2) was consistent with generators on the lateral surface of the temporal lobes (i.e., radial N1). Likewise, the target-related N2/P3 ERP sequence was evidenced by a frontocentral sink (*241*; Figure 3b, column 3), followed by a parietal P3b source (*343*; Figure 3b,

Table 2. *Comparison of Varimax–Rotated CSD–PCA Solutions for Novelty, Dichotic, and Binaural Oddball Tasks*

Novelty oddball[a]		Dichotic oddball[b,c]		Binaural oddball[b,d]		Identifying sink (–) and source (+) activity	
Peak latency (ms)	Explained variance (%)	Peak latency (ms)	Explained variance (%)	Peak latency (ms)	Explained variance (%)	Targets	Novels
120	3.49	105	4.8	105	4.5	N1 –	
179	4.66	150	2.3	160	3.9	temporal N1 –	novelty N2 –
241	6.95	245	3.6	215	5.3	N2 –	novelty vertex+
343	17.49	440	30.3	355	23.0	P3b+; frontal P3+	P3b+; frontal P3+
542	25.71	620	14.9	560	24.0	F – C+	
956	30.10	885	26.3	920	25.6	"ASW"/noise variance	

Note: Only novelty N2 and novelty vertex + are unique to novel stimuli.
[a]67-channel CSD.
[b]31-channel CSD.
[c]Tenke et al. (2008).
[d]Kayser and Tenke (2006b).

column 4), with an asymmetric, right-sided extension into temporal lobe regions. Finally, the distinctive, target-specific, late positivity corresponding to the characteristic midfrontal sink/centroparietal source factor, F − CP + (*542*; Figure 3b, column 5) was identified. The remaining high-variance component (*956*; often identified as "slow wave" to reflect the loadings' time course) represents slow, task-irrelevant variance that is largely attributable to the baseline correction procedure (Section 1.3 of Kayser & Tenke, 2003).

Despite this degree of consistency with the CSD-PCA factor structure produced in other oddball tasks, there were notable differences. Compared to the other tasks using tonal stimuli, the target N2 sink (*241*) was shifted medially, with maximal sink amplitude at the frontal midline (Figure 3b, column 3, factor *241*). The frontal P3 source was only observed for the novelty oddball task, and was concurrent with parietal P3b (*343*; Figure 3b, row 2, column 4, factor *343*). Although the frontal P3 source (*343*) was also present for novel stimuli, the only P3 source that was unique to novel stimuli was the novelty vertex source (factor *241*; Figure 3b, row 3, column 3; Table 2), which was preceded by a midline novelty N2 sink.[3]

Statistical methods

The focus of the present study was on the novelty P3, which has a well-documented midline topography. Our reliance on CSD waveforms eliminates quantitative and statistical ambiguities caused by the choice of a recording reference, while sharpening and enhancing these midline topographies, thereby simplifying measurements and comparisons between groups. Moreover, the distinctive pattern of localized sources and sinks observed in the novelty oddball task indicate qualitative differences across conditions (cf. Figure 3b, factors *241*, *343*, and *542*). For this reason, separate repeated measures analyses of variance (ANOVAs; BMDP-4V; Dixon, 1992) were conducted for the sources underlying the late positivities to targets and novels using subsets of electrode sites corresponding to these characteristic topographies. Greenhouse–Geisser ε correction was applied when appropriate (e.g., Keselman, 1998).

In previous binaural and dichotic oddball tasks, we restricted our analysis of target-related P3b sources to parietal sites (e.g., Kayser & Tenke, 2006b; Tenke et al., 2008; but for an alternative, see Kayser, Tenke, Gates, & Bruder, 2007). In the present study, the target P3b source (*343*) was best defined at the five medial parietal sites (Pz, P1/2, P3/4). However, this source topography extended into lateral sites, requiring an additional ANOVA to probe source asymmetries using seven homologous pairs (TP7/8, P7/8, P5/6, P3/4, P1/2, PO7/8, PO3/4). The corresponding midfrontocental source of factor *343* consisted of four sites: AFz, Fz, F1/2. Finally, F − CP+ (*542*) was measured at five sites for the mid-frontocental sink (FCz, Fz, F1/2, FCz) and four homologous pairs for the centroparietal source (CP1/2, CP3/4, P1/2, P3/4). In addition to these regions, the novelty response also included a novelty vertex source for factor *241* (FCz, Cz, C1/2, CPz), and a secondary lateral frontal source topography (AF7/8, F7/8). ANOVA models for each of the midline topographies included group (patient, control) as a between-subjects factor and site (all electrode sites within the region) as a within-subject factor, or hemisphere (left, right) and site for topographies displaced from the midline. Even though the age difference between groups was small, significant ANOVA results were confirmed using age as a covariate.

To assure the adequacy and stability of the temporal CSD-PCA solution, CSD waveforms were also subjected to a temporal PCA restricted to novels in the first versus last half of trials, as well as a hemispatial PCA (Tenke et al., 2008). Results were consistent with those from the overall temporal CSD-PCA and are not further detailed here (see Supplemental Material).

Comparison with CSD-PCA Solution for 31-Channel Data

Our previous study (Bruder, Kroppmann, et al., in press) reported findings of nose-referenced ERPs from a 31-channel montage (Grass amplifiers using a 0.1–30-Hz band pass) at 200 samples/s in 20 healthy controls and 20 depressed patients. All participants were right-handed, and the groups did not significantly differ in age or education level. CSD-PCA were also computed from these data for this report, using the 241 time points as variables (− 200 to 1000 ms), with a total of 3,720 observations consisting of three conditions (novel, target, nontarget), 40 subjects, and 31 sites (electrodes). The comparability of CSD-PCA solutions for this initial study and the current replication was evaluated by comparing rotated factor loadings and factor score topographies.

Results

Behavioral Performance

Participants performed well on this task (98.5 ± 1.9 total% correct). Only one healthy participant and five depressed patients performed at less than 95%. Nontarget performance was close to perfect for both groups (controls: 99.6 ± 0.6; patients: 99.5 ± 0.8), and the correct rejection of novels was comparable for the two groups (controls: 96.6 ± 4.3; patients: 96.4 ± 4.2). Patients had significantly longer reaction times to targets compared to controls (491 ± 87 ms vs. 438 ± 88 ms), $F(1,97) = 8.84$, $p = .004$, a difference that was preserved when age was used as a covariate, $F(1,97) = 5.62$, $p = .02$.

CSD-PCA Comparisons between Groups

Figure 4 shows CSD waveforms for healthy controls and depressed patients at midline sites, with reference lines fixed at latencies corresponding to loadings peaks for factors *179*, *241*, *343*, and *542*. Although nontarget N1 and P2 are comparable for the two groups, target-related differences are distributed over time and invert along the midline from a posterior source reduction (at Pz) to an anterior source enhancement (AFz, Fz) in patients (Figure 4, column 2). However, the group difference in response to novels was quite localized, being greatest at vertex (Cz), where a prominent sink (*179* ms) was followed by a source (*241* ms) in both groups. Although the amplitude of the sink was comparable in the two groups, the novelty vertex source was markedly reduced in patients. The amplitude of the subsequent novelty response at frontal sites (*343* ms) did not differ between groups.

Figure 5 reveals that factor score topographies were similar in patients and controls for nontarget and target stimuli. The novelty vertex source (*241*) was unique to novels and showed a prominent reduction in depressed patients. In contrast, the midline frontal P3 source (*343*) topography was not unique to novels (i.e., was also prominent for targets), and was equally evident in patients and controls.

[3]We refer to this *179* sink with the functional term "novelty N2 sink" to avoid confusion with MMN generators in the temporal lobe.

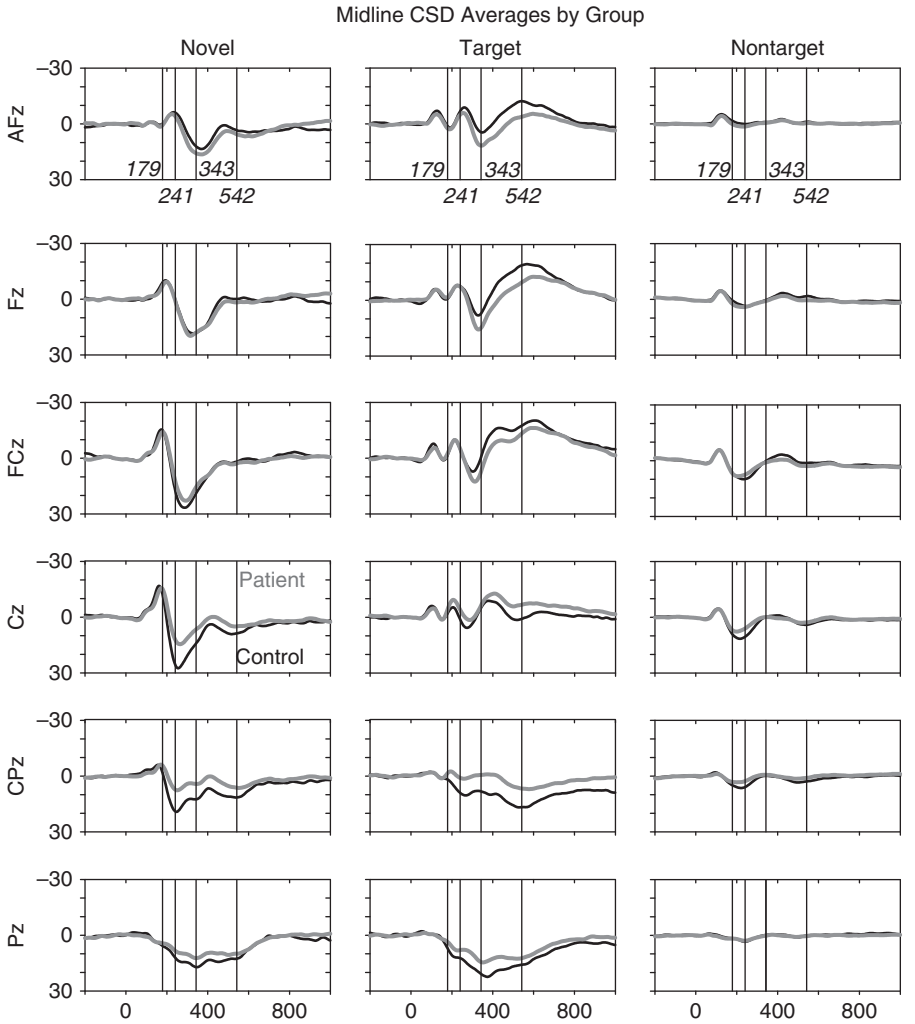

Figure 4. Averaged midline CSD waveforms for depressed patients (bold gray) and healthy controls (black) for novels (left column), targets (center), and nontargets (right). Vertical lines indicate peak latencies of CSD-PCA factors of interest (labeled in AFz waveforms). For novels, a short latency sink (novelty N2) is followed by a source (novelty P3) at central sites (CPz, Cz), both of which are attenuated and delayed at anterior sites, where the peak latency approximates that observed for target P3. Scale: negative-up (sink).

Statistical Analyses

Target sources. Significant ANOVA results for target and novel stimuli are shown in Table 3 for factors *241*, *343*, and *542*. Evidence suggesting midparietal source reduction and midfrontal P3 source enhancement for *343* in patients (cf. Figure 5, column 2) was not preserved when age was included as a covariate. A notable P3b asymmetry at lateral temporoparietal sites was also unrelated to group. However, the midfrontal response-related sink (*542*) was significantly reduced in patients, the corresponding centroparietal source being reduced at sites CP1/2, and larger over the left than right hemisphere.

Novelty sources. The prominent, novelty vertex source (*241*) was markedly reduced in patients (cf. Table 3 and Figure 5, column 1), and was preserved when age was used as a covariate as well as after age differences were eliminated by excluding the 26 oldest participants, $F(1,70) = 4.232$, $p = .04$. This group difference did not reflect activity in the secondary, frontal source of factor *241*, which showed an effect in the opposite direction. In marked contrast, the subsequent P3 source (*343*) did not differ between groups for novel stimuli, either at midfrontal or posterior sites.

Source Correlations with Age, Performance, and Clinical Features

Table 4 shows the correlations of the regional mean source amplitudes with age and task performance. Age was most strongly correlated with the factor score amplitudes for the target P3 source (*343*) and the novelty vertex source (*241*), with larger sources in younger subjects. This observation confirms the importance of age as a covariate in the reported analyses. Performance measures were significantly correlated with target-related parietal P3 (*343*: RT and hit rate) and the response-related centroparietal source (*542*: RT only), as well as the novelty vertex source (*241*: hit rate only).

Severity of depression on the BDI was significantly correlated with the novelty vertex source ($r = -.30$, $n = 94$, $p = .003$) as well as the late response-related source ($r = -.28$, $n = 94$, $p = .006$). However, the association was presumably due to the patient/control classification, as it was not supported when controls were excluded. In contrast, the Chapman measure of physical anhedonia (Chapman & Chapman, 1978) was significantly

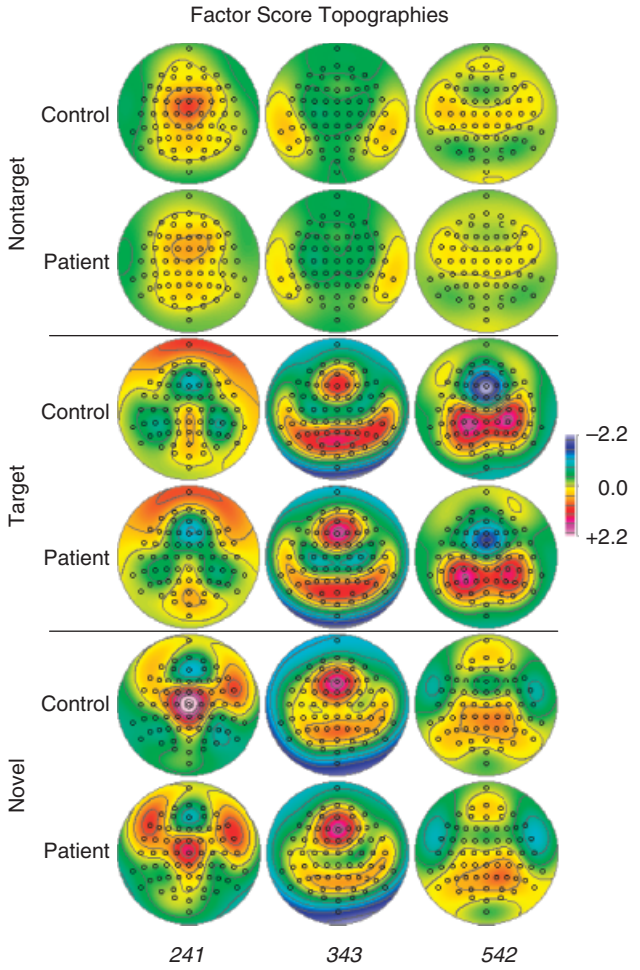

Figure 5. Averaged CSD-PCA factor score topographies for the first six factors in each group for nontargets (top), targets (middle), and novels (bottom). Factors are indicated below by peak latency. The early midline *179* sink/*241* source pattern is unique to novel stimuli, as is the reduction of the early *241* source in patients. Scale: blue sink, red source.

correlated with the response-related source (*542*), both across all participants ($r = -.25$, $n = 89$, $p = .02$) and for patients alone ($r = -.32$, $n = 43$, $p = .04$).

Table 4. *Correlations of Mean Regional Source Amplitude with Age and Performance*

Stimulus (factor)	Region	Age ($n = 98$)	Hit rate ($n = 98$)	Mean RT ($n = 98$)
Target (*343*)	parietal source	−.41**	.26*	.57**
	Fz source	.16	.17	.14
Target (*542*)	CP source	−.21*	.09	−.38**
Novel (*241*)	vertex source	−.44**	.29**	−.18
Novel (*343*)	Fz source	−.07	.19	.07

*$p < .05$, **$p < .01$.

Replication in an Independent Sample

Figure 6 shows grand mean CSD waveforms for 67-channel and 31-channel studies at midline sites. In both studies, the target P3b source was largest at Pz, and the novelty vertex source was earlier and larger than the novelty source at frontal sites. Consequently, the CSD-PCA extracted factors with highly comparable loadings (Figure 7a) and factor score topographies (Figures 5 and 7b), including a prominent novelty vertex source factor unique to novels that was reduced in patients. Likewise, the response-related F − CP+component (*500*) was more prominent in controls, particularly for the midline frontal sink. However, parietal P3 was more prominent for controls in the 31-channel study (Figure 6), both for targets and novels (*335*, Figure 7b).

Discussion

Novelty P3 and the CSD-PCA Factor Structure for the Novelty Oddball Task

The basic CSD-PCA factor structure for the novelty oddball task agrees with that observed for other oddball tasks. Factors with comparable topographies for all classes of stimuli included N1, a bilateral sink/source pair consistent with activation of primary auditory cortex within the Sylvian fissure, followed by temporal N1, a bilateral sink topography consistent with generators on the lateral surface of the temporal lobes. Target-related factors included N2 (lateral and midline frontal sinks), P3b (parietal source), and a later, response-related factor (F − CP+) that cor-

Table 3. *Significant Repeated Measures ANOVA Effects for CSD-PCA Factors of Interest*

			ANOVA				With age covariate			
Stimulus (factor)	Region (sites)	Effect	*F*	*df*	ε	*p*	*F*	*df*	ε	*p*
Target (*343*)	Midparietal source (Pz, P1/2, P3/4)	Group	5.86	1,96		.02	2.74	1,95		.10
	Lateral temporoparietal source (TP7/8, P7/8, P5/6, P3/4, P1/2, PO7/8, PO3/4)	Hemisphere × Site[a]	4.61	6,576	.46	.005	3.03	6,570	.46	.03
	Midfrontal source (AFz, Fz, F1/2)	Group	4.51	1,96		.04	3.26	1,95		.07
Target (*542*)	Midfrontal sink (FCz, Fz, F1/2, FCz)	Group	7.54	1,96		.001	4.46	1,95		.04
	Centroparietal source (CP1/2, CP3/4, P1/2, P3/4)	Hemisphere	11.63	1,96		.001	.91	1,95		n.s.
		Group × Site[b]	4.95	3,288	.76	.002	3.17	3,285	.76	.04
Novel (*241*)	Vertex source (FCz, Cz, C1/2, CPz)	Group	7.98	1,96		.006	4.16	1,95		.04
	Lateral frontal source (AF7/8, F7/8)	Group	7.38	1,96		.008	3.63	1,95		.06
		Hemisphere × Site[c]	21.67	1,96		.000	6.40	1,95		.01

Note: Interactions including site as a factor were followed up by simple effects at each site.
[a]Hemisphere simple effect only at site TP7/8, $F(1,96) = 9.89$, $p = .002$, and P5/6, $F(1,96) = 4.37$, $p = .04$.
[b]Group simple effect only at sites CP1/2, $F(1,96) = 6.73$, $p = .01$.
[c]Hemisphere simple effect only at site F7/8, $F(1,96) = 12.10$, $p = .001$.

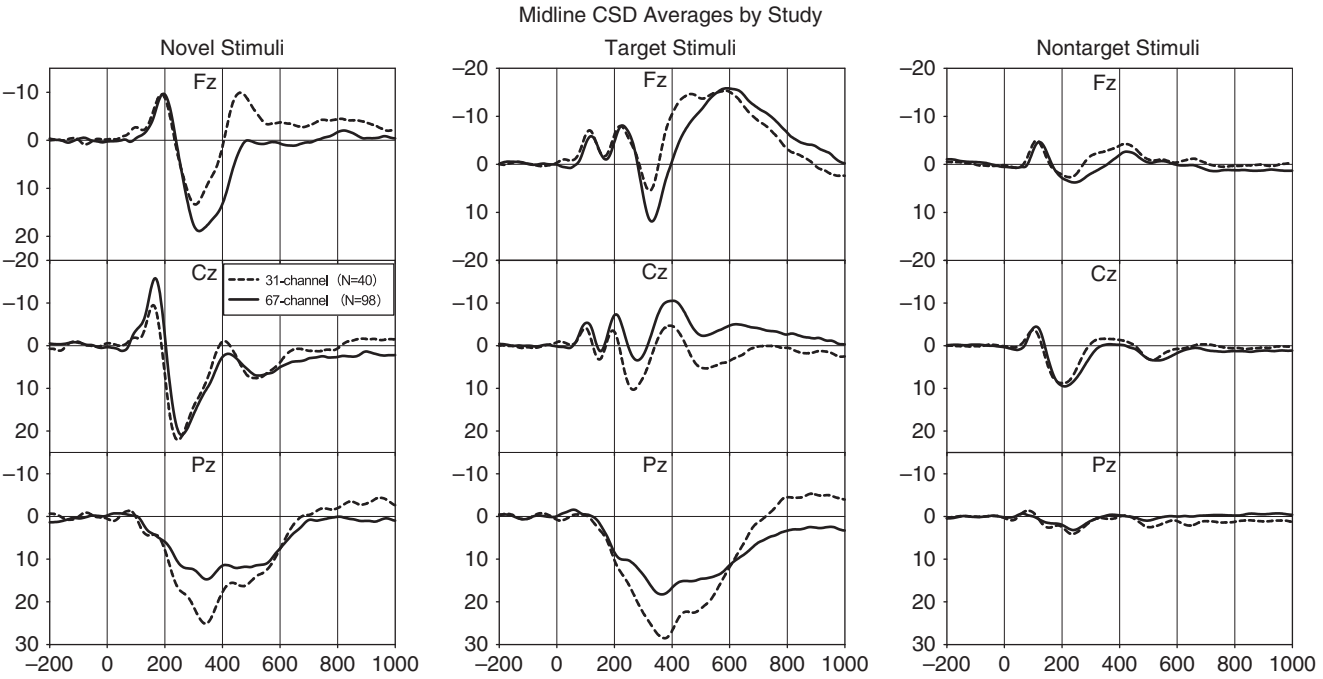

Figure 6. Across-study comparison of averaged midline CSD waveforms at Fz, Cz, and Pz for depressed patients and healthy controls for novels (left column), targets (center), and nontargets (right). Solid line: 67-channel study; dashed lines: previous 31-channel study. Despite amplitude differences, components were generally comparable in each study. Scale: negative-up (sink).

responds to a frontally inverting, slow wave contribution of the late positive complex, and that resembles a spatial factor described by Spencer, Wijesinghe, Dien, and Donchin (1999).

Despite the general comparability of CSD-PCA solutions across oddball tasks, there were notable target-related differences between components in the novelty task as compared with other oddball tasks using tonal stimuli. First, rather than overlying the lateral surface of the frontal lobes, the topography of the target-related N2 sink was largely confined to midline frontal sites. Second, the target-related P3 source included a secondary topography at the same midline frontal sites, rather than being restricted to a parietal P3b topography. These target-related characteristics presumably reflect the changed expectancies in the novelty oddball task, in which target likelihood was reduced (.12 compared to .2) and a class of novel nontargets (distracters) was added. These differential characteristics were replicable across recording systems and evident regardless of whether a low- or high-density montage was used. They cannot be attributed to false alarms, because only correct trials were included in the averaged waveforms. Task difficulty can also be ruled out, as they were not observed in a more difficult dichotic oddball task (Tenke et al., 2008). Although the novelty oddball task differed in stimulus timing (1-s SOA as compared to 2 s for the previous two-stimulus oddball tasks), the topography of the later response-related factor (F − CP+) was preserved for both groups, indicating that any variations in component structure that were related to the abbreviated response period were resolved by the end of the epoch.

The response to novel stimuli was characterized by the expected midline frontocentral P3 source, both in patient and control groups. However, CSD-PCA separated an additional source contributing to the midline novelty P3: the novelty vertex source (*241*), which was present only for novels, and was distinct from a later frontal source (*343*) having the same latency and topography as observed for targets. This source is evidenced in ERP waveforms as an inflection on the rising phase of the novelty P3 (cf. Figure 1, midline sites at latencies following nontarget P2) and accords well with findings by Yago, Escera, Alho, Giard, and Serra-Grabulosa (2003), who also reported an early central source "before the onset of the [novelty P3] waveform, contributing solely to its early phase" (p. 383).

The early novelty source was preceded by an equally well-defined novelty N2 sink (*179*) at precisely the same sites that was not observed for targets. It is, therefore, this sink/source pair (i.e., *179*/*241*) that best qualifies as a substrate for the response to novelty. To the extent that the novelty vertex source defines onset of the volume-conduced ERP at the midline, its differential engagement could contribute to, or even account for, the characteristic early onset of novelty P3, as well as its topographic shift with repetition (Friedman & Simpson, 1994). In contrast, the fact that the frontal P3 source for targets is comparable to that observed for novels precludes a unique role for this later frontal source in the automatic attentional response to novelty. To the contrary, the focal novelty vertex source suggests a more posterior generator (i.e., in or behind SMA),[4] which is consistent with the localization of an equivalent dipole for go/no-go P3 in portions of cingulate cortex near motor areas (Verleger et al., 2006), and is a location more consistent with processes related to response inhibition than with task-specific stimulus classification or error processing per se.

[4]It should also be acknowledged that the novelty vertex source factor has a complex, anterior, secondary topography, composed of an anterior sink and frontolateral sources, that suggests an additional deep generator.

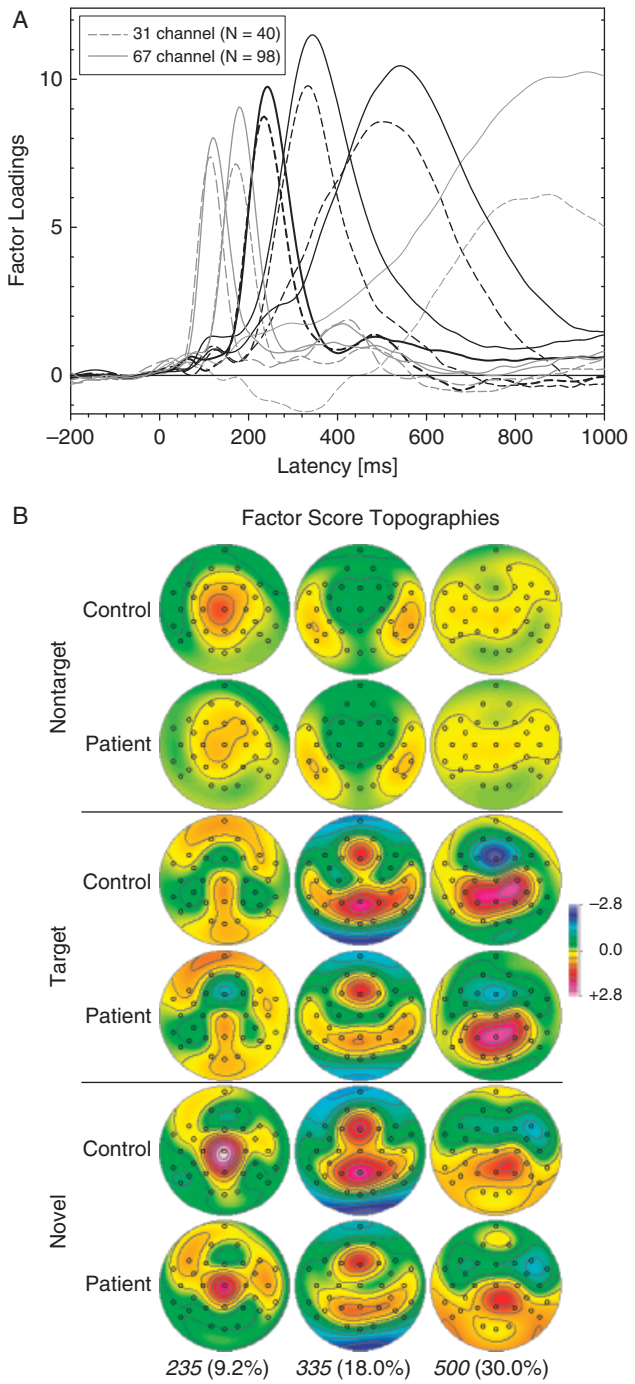

Figure 7. Comparison of unrestricted temporal PCA solutions for CSD waveforms in the two studies. A: Corresponding factor loadings waveforms for 67-channel (solid) and 31-channel (dashed) studies. Factors are unambiguous, despite minor waveform variations in morphology and relative amplitudes. Bold lines indicate the three factors representing the late positive complex. B: Factor score topographies of the three factors representing the late positive complex from the 31-channel study for correct nontargets, targets, and novels. Factors are identified by peak latency and percent of variance accounted for (in parentheses). Scale: blue sink, red source.

PCA and independent components analysis (ICA) have previously been used to distinguish between P3 subcomponents in the novelty oddball task. One ERP-PCA study (Strobel et al., 2004) also separated an early (240 ms) from late (324 ms) novelty P3. This study further distinguished an even later positivity (492 ms, but identified as P3b), which presumably corresponds to our late, response-related CSD-PCA factor (i.e., F – CP+). Moreover, CSD maps derived from early novelty P3 had a more posterior (i.e., central midline) topography than was obtained for the late component. Debener et al. (2005) used ICA to further explore the class of novel stimuli. They evaluated the impact of using novels as nontargets in an ongoing target detection task (in their case, silent count) by comparing the ERP response to that obtained when novels were targets. Trial-by-trial ERPs were submitted to ICA, which separated an anterior from a posterior cluster. The anterior cluster corresponded, in part, to a midline frontocentral novelty P3, whereas the posterior cluster reflected aspects of parietal P3b. As reflected in single-trial and split-half plots, nontarget novelty P3 in the frontocentral cluster decreased over trials, the decreases being most prominent at latencies longer than the novelty P3 peak. In contrast, when novels were used as targets, frontocentral P3 was generally enhanced, with no evidence of habituation.

Using insights from spatiotemporal PCA, Spencer et al. (2001) emphasized the importance of preserving a common nomenclature for putative ERP components based on their functional and topographic properties. Noting that novels produce both a posterior P3 and a frontal novelty P3, they concluded that the ERP topography produced to novels in any task reflects the summation of task-related contributions from each component. Inasmuch as this summation is largely due to volume conduction from anatomically distinct generators, it follows that these contributions may be better separated by CSD. We strongly concur regarding the importance of topography for component identification and further note that the sharpened topographies of CSD-PCA components allow the distinction of an earlier (factor *241*) novelty vertex source from the later and less well-localized frontal and parietal P3 sources (i.e., factor *343*). Although the later sources are generally identified as novelty P3 (P3a) and P3b (target P3), respectively, the time course and central topography of the earlier novelty vertex source clearly contribute to the early phase and midline topography of the novelty ERP.[5] These findings are directly apparent from the raw waveforms (Figure 4), replicable across studies, equally evident for early and late trials (Supplementary Figure S1), and consistent regardless of whether a temporal or a hemispatial PCA was computed (Supplementary Figure S2). Given that the earlier novelty P3 source satisfies the three main criteria of the ERP component construct, consisting of both a distinctive neuroanatomical origin and time course (i.e., spatial and temporal characteristics) with an amplitude influenced by experimental manipulation, we identify it as a distinct component, the novelty vertex source (NVS).

Novelty P3 and Depression

The novelty P3 source was localizable to the midline frontocentral region along the longitudinal fissure and was markedly reduced in depressed patients when compared to healthy controls. Previous work suggests that this reduction reflects a deficit in an early attentional response to novelty, rather than in the later cognitive evaluation of these stimuli. However, the novelty P3 reduction was

[5]We have identified the early novelty vertex source as novelty P3 based on functional considerations and in conformance with previous studies. However, the short latency and central topography of this component are both suggestive of P2, which is separable from N1 and has been distinguished from NoGo-P3 (Crowley & Colrain, 2004).

restricted to the earliest phase of the source at the vertex. In contrast, the subsequent, frontal portion of the midline source, characterizing both target and novel stimuli in this task, was not reduced.

In addition to the novelty vertex source, the response-related F – CP+, which corresponds to a late frontally inverting positivity, was also reduced in patients. This late source was negatively correlated with self-ratings of both depression (BDI) and physical anhedonia. It presumably reflects a response-related deficit, possibly owing to patients with melancholic or anhedonic forms of depression (see also Bruder et al., 1991).

Dysfunction of frontal cortex, and particularly the ACC, has been reported in depressed patients using imaging techniques (Bremner, Vythilingam, Vermetten, Vaccarino, & Charney, 2004; Drevets et al., 1997; Siegle, Steinhauer, & Thase, 2004), consistent with an attentional impairment. However, a similarity between P3a and no-go P3 produced in a go/no-go task (Polich, 2007) suggests the possibility that parallel findings in novelty oddball and executive control paradigms may result from common neuroanatomical mechanisms that underlie attentional control, response selection, and/or response inhibition. The present findings of an early source reduction in depression for novels (i.e., responses correctly inhibited) may thereby be related to the reported no-go performance decrement in depression (Kaiser et al., 2003) and to a reduction in no-go P3 (Ruchsow et al., 2008). If the early central novelty source actually reflects inhibition of a task-specific response to irrelevant stimuli, it would suggest that a motor, rather than an attentional, process is impaired in depression. However, inhibition in the novelty oddball task could extend well beyond the task-specific behavioral response, to encompass autonomic/affective aspects of the orienting response as well. This broadened conceptualization accords well with evidence suggesting a correspondence between frontocentral novelty P3 (but not P3b) and electrodermal evidence of an orienting response as well as the elimination of this association after mild alcohol intoxication (Marinkovic et al., 2001).

CSD-PCA Topographies as Constraints on Deep Generators

Methods for identifying neuronal generators underlying a scalp-recorded ERP rely on the volume-conduction relation expressed by Equation (1). Traditionally, scalp topographies have been used to suggest generators, but the task is hampered by the blurring introduced by volume conduction itself. Scalp-CSD sharpens these topographies and reexpresses them in terms of effective radial current generators from subjacent anatomical regions and thereby provides constraints on possible generators. Inverse models (e.g., BESA, LORETA) can improve this anatomical specificity by implementing additional assumptions to allow for stable or plausible solutions, such as the reasonable presupposition of continuity. However, the partial closure of intracranial fields is characterized by abrupt field transitions (Tenke et al., 1993). Invasive methods provide stronger evidence for generators (e.g., intracranial CSD profiles), but even these may require additional evidence before their laminar and cellular mechanisms may be deduced (Schroeder et al., 1995). Convergent evidence from other sources (e.g., functional imaging) may also be useful, but only as it illuminates the relationship expressed in Equation (1).

Midline ERP generators have been inferred for phenomena spanning a range of cognitive and spectral paradigms (e.g., ERN/theta: Luu, Tucker, & Makeig, 2004; EEG/theta: Gevins & Smith 2000; McEvoy, Pellouchoud, Smith, & Gevins, 2001; Pizzagalli et al., 2001; but see Tenke & Kayser, 2005). There may even be a fundamental link between midline theta and novelty P3 (Demiralp, Ademoglu, Comerchero, & Polich, 2001; Isler, Grieve, Czernochowski, Starkm, & Friedman, 2008). Relevant for all these findings is that a single pair of bilaterally symmetric, midline dipoles (e.g., ACC simulation) produces sufficient field closure to impede inverse solutions (Tenke & Kayser, 2008). However, the same simulated generator produces a scalp-CSD topography that correctly describes deep sinks projecting bilaterally from the midline over the lateral frontal lobe, with uncanceled sources aligned narrowly along the overlying frontal midline (e.g., Kayser & Tenke, 2006b; Tenke & Kayser, 2005, 2008). This precise CSD pattern has also been observed in word recognition memory tasks, revealing old–new effects for a response-locked midfrontal sink with significant effects corresponding to this topography (Kayser et al., 2007). It follows, therefore, that CSD-PCA provides a comprehensive, yet conservative, linear approach for identifying and quantifying the generator patterns underlying the scalp-recorded ERP.

REFERENCES

Alexander, J. E., & Polich, J. (1995). P300 differences between sinistrals and dextrals. *Cognitive Brain Research*, *2*, 277–282.

Anokhin, A. P., Vedeniapin, A. B., Sirevaag, E. J., Bauer, L. O., O'Connor, S. J., Kuperman, S., et al. (2000). The P300 brain potential is reduced in smokers. *Psychopharmacology*, *148*, 409–413.

Baudena, P., Halgren, E., Heit, G., & Clarke, J. M. (1995). Intracerebral potentials to rare target and distractor auditory and visual stimuli. III. Frontal cortex. *Electroencephalography and Clinical Neurophysiology*, *94*, 251–264.

Beck, A. T., Ward, C. H., Mendelson, M., & Erbaugh, J. (1961). An inventory for measuring depression. *Archives of General Psychiatry*, *4*, 561–571.

BioSemi, Inc. (2001). *ActiveTwo—Multichannel, DC amplifier, 24-bit resolution, biopotential measurement system with active electrodes.* Amsterdam, Netherlands: Author. (http://www.biosemi.com)

Bremner, J. D., Vythilingam, M., Vermetten, E., Vaccarino, V., & Charney, D. S. (2004). Deficits in hippocampal and anterior cingulate functioning during verbal declarative memory encoding in midlife major depression. *American Journal of Psychiatry*, *161*, 637–645.

Bruder, G. E., Kayser, J., & Tenke, C. E. (in press). Event-related brain potentials in depression: Clinical, cognitive and neurophysiologic implications. In S. J. Luck & E. S. Kappenman (Eds.), *Event-related potential components: The ups and downs of brainwave recordings*. New York: Oxford University Press.

Bruder, G. E., Kayser, J., Tenke, C. E., Leite, P., Schneier, F. R., Stewart, J. W., et al. (2002). Cognitive ERPs in depressive and anxiety disorders during tonal and phonetic oddball tasks. *Clinical Electroencephalography*, *33*, 119–124.

Bruder, G. E., Kroppmann, C. J., Kayser, J., Stewart, J. W., McGrath, P. J., & Tenke, C. E. (in press) Reduced brain responses to novel sounds in depression: An electrophysiological study. *Psychiatry Research* (in press).

Bruder, G. E., Tenke, C. E., Stewart, J. W., Towey, J. P., Leite, P., Voglmaier, M., et al. (1995). Brain event-related potentials to complex tones in depressed patients: Relations to perceptual asymmetry and clinical features. *Psychophysiology*, *32*, 373–381.

Bruder, G. E., Towey, J. P., Stewart, J. W., Friedman, D., Tenke, C., & Quitkin, F. M. (1991). Event-related potentials in depression: Influ-

ence of task, stimulus hemifield and clinical features on P3 latency. *Biological Psychiatry*, *30*, 233–246.
Chapman, L. J., & Chapman, J. P. (1978) Revised Physical Anhedonia Scale. (Available from L. J. Chapman, Department of Psychology, 1202 West Johnson Street, University of Wisconsin, Madison, WI 53706, USA).
Courchesne, E., Hillyard, S. A., & Galambos, R. (1975). Stimulus novelty, task relevance and the visual evoked potential in man. *Electroencephalography and Clinical Neurophysiology*, *39*, 131–143.
Crottaz-Herbette, S., & Menon, V. (2006). Where and when the anterior cingulate cortex modulates attentional response: Combined fMRI and ERP evidence. *Journal of Cognitive Neuroscience*, *18*, 766–780.
Crowley, K, E., & Colrain, I. M. (2004). A review of the evidence for P2 being an independent component process: Age, sleep and modality. *Clinical Neurophysiology*, *115*, 732–744.
Debener, S., Makeig, S., Delorme, A., & Engel, A. K. (2005). What is novel in the novelty oddball paradigm? Functional significance of the novelty P3 event-related potential as revealed by independent component analysis. *Cognitive Brain Research*, *22*, 309–321.
Demiralp, T., Ademoglu, A., Comerchero, M., & Polich, J. (2001). Wavelet analysis of P3a and P3b. *Brain Topography*, *13*, 251–267.
Dien, J., Spencer, K. M., & Donchin, E. (2003). Localization of the event-related potential novelty response as defined by principal components analysis. *Cognitive Brain Research*, *17*, 637–650.
Dixon, W. J. (Ed.). (1992). *BMDP statistical software manual: To accompany the 7.0 software release*. Berkeley, CA: University of California Press.
Donchin, E. (1966). A multivariate approach to the analysis of average evoked potentials. *IEEE Transactions on Biomedical Engineering*, *13*, 131–139.
Drevets, W. C., Price, J. L., Simpson, J. R. Jr., Todd, R. D., Reich, T., Vannier, M., et al. (1997). Subgenual prefrontal cortex abnormalties in mood disorders. *Nature*, *386*, 824–827.
First, M. B., Spitzer, R. L., Gibbon, M., & Williams, J. B. W. (1996). *Structured clinical interview for DSM-IV Axis I disorders—Nonpatient edition (SCID-NP)*. New York: Biometrics Research Department, New York State Psychiatric Institute.
Friedman, D., Cycowicz, Y. M., & Gaeta, H. (2001). The novelty P3: An event-related brain potential (ERP) sign of the brain's evaluation of novelty. *Neuroscience and Biobehavioral Reviews*, *25*, 355–373.
Friedman, D., & Simpson, G. V. (1994). ERP amplitude and scalp distribution to target and novel events: Effects of temporal order in young, middle-aged and older adults. *Cognitive Brain Research*, *2*, 49–63.
Friedman, D., Simpson, G., & Hamberger, M. (1993). Age-related changes in scalp topography to novel and target stimuli. *Psychophysiology*, *30*, 383–396.
Gevins, A., & Smith, M. E. (2000). Neurophysiological measures of working memory and individual differences in cognitive ability and cognitive style. *Cerebral Cortex*, *10*, 829–839.
Glaser, E. M., & Ruchkin, D. S. (1976). *Principles of neurobiological signal analysis*. New York: Academic Press.
Halgren, E., Baudena, P., Clarke, J. M., Heit, G., Liegeois, C., Chauvel, P., et al. (1995). Intracerebral potentials to rare target and distractor auditory and visual stimuli. I. Superior temporal plane and parietal lobe. *Electroencephalography and Clinical Neurophysiology*, *94*, 191–220.
Halgren, E., Marinkovic, K., & Chauvel, P. (1998). Generators of the late cognitive potentials in auditory and visual oddball tasks. *Electroencephalography and Clinical Neurophysiology*, *106*, 156–164.
He, B., Lian, J., Spencer, K. M., Dien, J., & Donchin, E. (2001). A cortical potential imaging analysis of the P300 and novelty P3 components. *Human Brain Mapping*, *12*, 120–130.
Isler, J. R., Grieve, P. G., Czernochowski, D., Starkm, R. I., & Friedman, D. (2008). Cross-frequency phase coupling of brain rhythms during the orienting response. *Brain Research*, *1232*, 163–172.
Kaiser, S., Unger, J., Kiefer, M., Markela, J., Mundt, C., & Weisbrod, M. (2003). Executive control deficit in depression: Event-related potentials in a go/nogo task. *Psychiatry Research*, *122*, 169–184.
Kayser, J. (2003). *Polygraphic recording data exchange—PolyRex*. New York: New York State Psychiatric Institute, Department of Biopsychology (http://psychophysiology.cpmc.columbia.edu/PolyRex.htm).
Kayser, J., & Tenke, C. E. (2003). Optimizing PCA methodology for ERP component identification and measurement: Theoretical rationale and empirical evaluation. *Clinical Neurophysiology*, *114*, 2307–2325.
Kayser, J., & Tenke, C. E. (2005). Trusting in or breaking with convention: Towards a renaissance of principal components analysis in electrophysiology. *Clinical Neurophysiology*, *116*, 1747–1753.
Kayser, J., & Tenke, C. E. (2006a). Electrical distance as a reference-free measure for identifying artifacts in multichannel electroencephalogram (EEG) recordings. *Psychophysiology*, *43*, S51.
Kayser, J., & Tenke, C. E. (2006b). Principal components analysis of Laplacian waveforms as a generic method for identifying ERP generator patterns: I. Evaluation with auditory oddball tasks. *Clinical Neurophysiology*, *117*, 348–368.
Kayser, J., & Tenke, C. E. (2006c). Principal components analysis of Laplacian waveforms as a generic method for identifying ERP generator patterns: II. Adequacy of low-density estimates. *Clinical Neurophysiology*, *117*, 369–380.
Kayser, J., Tenke, C. E., Gates, N. A., & Bruder, G. E. (2007). Reference-independent ERP old/new effects of auditory and visual word recognition memory: Joint extraction of stimulus- and response-locked neuronal generator patterns. *Psychophysiology*, *44*, 949–967.
Keselman, H. J. (1998). Testing treatment effects in repeated measures designs: An update for psychophysiological researchers. *Psychophysiology*, *35*, 470–478.
Klee, M., & Rall, W. (1977). Computed potentials of cortically arranged populations of neurons. *Journal of Neurophysiology*, *40*, 647–666.
Knight, R. T. (1984). Decreased response to novel stimuli after prefrontal lesions in man. *Electroencephalography and Clinical Neurophysiology*, *59*, 9–20.
Kroppmann, C. J., Tenke, C. E., Kayser, J., Sedoruk, J. P., Griggs, C. B., Stewart, J. W., et al. (2006). Brain responses to novel sounds in depression: An ERP study. *Psychophysiology*, *43*, S55.
Lorente de No, R. A. (1947). *A study of nerve physiology* (Rockefeller Institute for Medical Research, study 132 (pp. 389–477). New York: Rockefeller Institute.
Luu, P., Tucker, D. M., & Makeig, S. (2004). Frontal midline theta and the error-related negativity: Neurophysiological mechanisms of action regulation. *Clinical Neurophysiology*, *115*, 1821–1835.
Marinkovic, K., Halgren, E., & Maltzman, I. (2001). Arousal-related P3a to novel auditory stimuli is abolished by a moderately low alcohol dose. *Alcohol and Alcoholism*, *36*, 529–539.
Mathalon, D. H., Whitfield, S. L., & Ford, J. M. (2003). Anatomy of an error: ERP and fMRI. *Biological Psychology*, *64*, 119–141.
McEvoy, L. K., Pellouchoud, E., Smith, M. E., & Gevins, A. (2001). Neurophysiological signals of working memory in normal aging. *Cognitive Brain Research*, *11*, 363–376.
Mitzdorf, U. (1985). Current source-density method and application in cat cerebral cortex: Investigation of evoked potentials and EEG phenomena. *Physiological Review*, *65*, 37–100.
NeuroScan, Inc. (2003) *SCAN 4.3, Vol. II. EDIT 4.3: Offline analysis of acquired data*. Document number 2203, Revision D. El Paso, TX: Compumedics Neuroscan.
Nicholson, C. (1973). Theoretical analysis of field potentials in anisotropic ensembles of neuronal elements. *IEEE Transactions on Biomedical Engineering*, *20*, 278–288.
Nunez, P. L., & Srinivasan, R. (2006). *Electric fields of the brain: The neurophysics of EEG* (2nd ed). New York: Oxford University Press.
Oldfield, R. C. (1971). The assessment and analysis of handedness: The Edinburgh Inventory. *Neuropsychologia*, *9*, 97–113.
Perrin, F., Pernier, J., Bertrand, O., & Echallier, J. F. (1989). Spherical splines for scalp potential and current density mapping. *Electroencephalography and Clinical Neurophysiology*, *72*, 184–187.
Pivik, R. T., Broughton, R. J., Coppola, R., Davidson, R. J., Fox, N., & Nuwer, M. R. (1993). Guidelines for the recording and quantitative analysis of electroencephalographic activity in research contexts. *Psychophysiology*, *30*, 547–558.
Pizzagalli, D., Pascual Marqui, R. D., Nitschke, J. B., Oakes, T. R., Larson, C. L., Abercrombie, H. C., et al. (2001). Anterior cingulate activity as a predictor of degree of treatment response in major depression: Evidence from brain electrical tomography analysis. *American Journal of Psychiatry*, *158*, 405–415.
Polich, J. (2007). Updating P300: An integrative theory of P3a and P3b. *Clinical Neurophysiology*, *118*, 2128–2148.
Roth, W. T., Duncan, C. C., Pfefferbaum, A., & Timsit-Berthier, M. (1986). Applications of cognitive ERPs in psychiatric patients. In W. C. McCallum, R. Zappoli, & F. Denoth (Eds.), *Cerebral psycho-*

physiology: Studies in event-related potential (EEG Supplement 38, pp. 419–438). Amsterdam: Elsevier.
Ruchsow, M., Groen, G., Kiefer, M., Beschoner, P., Hermle, L., Ebert, D., et al. (2008). Electrophysiological evidence for reduced inhibitory control in depressed patients in partial remission: A go/nogo study. *International Journal of Psychophysiology*, *68*, 209–218.
Schroeder, C. E., Steinschneider, M. S., Javitt, D., Tenke, C. E., Givre, S. J., Mehta, A. D., et al. (1995). Localization and identification of underlying neural processes. In G. Karmos, M. Molnar, V. Csepe, I. Czigler, & J. E. Desmedt (Eds.), *Perspectives of Event-related Potentials in Research* (EEG Suppl 44, pp. 55–75). Amsterdam: Elsevier.
Siegle, G. J., Steinhauer, S. R., & Thase, M. E. (2004). Pupillary assessment and computational modeling of the Stroop task in depression. *International Journal of Psychophysiology*, *52*, 63–76.
Simons, R. F., Graham, F. K., Miles, M. A., & Chen, X. (2001). On the relationship of P3a and the novelty-P3. *Biological Psychology*, *56*, 207–218.
Spencer, K. M., Dien, J., & Donchin, E. (2001). Spatiotemporal analysis of the late ERP responses to deviant stimuli. *Psychophysiology*, *38*, 343–358.
Spencer, K. M., Wijesinghe, R., Dien, J., & Donchin, E. (1999). Prefrontal activity in oddball paradigms as measured by scalp current density. *Psychophysiology*, *36*, S111.
Squires, N. K., Squires, K. C., & Hillyard, S. A. (1975). Two varieties of long-latency positive waves evoked by unpredictable auditory stimuli in man. *Electroencephalography and Clinical Neurophysiology*, *38*, 387–401.
Strobel, A., Debener, S., Anacker, K., Müller, J., Lesch, K. P., & Brocke, B. (2004). Dopamine D4 receptor exon III genotype influence on the auditory evoked novelty P3. *NeuroReport*, *15*, 2411–2415.
Sutton, S., Braren, M., Zubin, J., & John, E. R. (1965). Evoked-potential correlates of stimulus uncertainty. *Science*, *150*, 1187–1188.
Sutton, S., & Ruchkin, D. S. (1984). The late positive complex: Advances and new problems. *Annals of the New York Academy of Sciences*, *425*, 1–23.
Tenke, C. E., & Kayser, J. (2001). A convenient method for detecting electrolyte bridges in multichannel electroencephalogram and event-related potential recordings. *Clinical Neurophysiology*, *112*, 545–550.
Tenke, C. E., & Kayser, J. (2005). Reference-free quantification of EEG spectra: Combining current source density (CSD) and frequency principal components analysis (fPCA). *Clinical Neurophysiology*, *116*, 2826–2846.
Tenke, C. E., & Kayser, J. (2008) ERP generators within the longitudinal fissure: Are putative inverses flawed? Program No. 872.28. 2008. Neuroscience Meeting Planner. Washington, DC: Society for Neuroscience. Available at: http://psychophysiology.cpmc.columbia.edu/mmedia/sfn2008/sfn2008.pdf
Tenke, C. E., Kayser, J., Fong, R., Leite, P., Towey, J. P., & Bruder, G. E. (1998). Response- and stimulus-related ERP asymmetries in a tonal oddball task: A Laplacian analysis. *Brain Topography*, *10*, 201–210.
Tenke, C. E., Kayser, J., Shankman, S. A., Griggs, C. B., Leite, P., Stewart, J. W., et al. (2008). Hemispatial PCA dissociates temporal from parietal ERP generator patterns: CSD components in healthy adults and depressed patients during a dichotic oddball task. *International Journal of Psychophysiology*, *67*, 1–16.
Tenke, C. E., Schroeder, C. E., Arezzo, J. C., & Vaughan, H. G. Jr. (1993). Interpretation of high- resolution current source density profiles: A simulation of sublaminar contributions to the visual evoked potential. *Experimental Brain Research*, *94*, 183–192.
Verleger, R., Paehge, T., Kolev, V., Yordanova, J., & Jaskowski, P. (2006). On the relation of movement-related potentials to the go/no-go effect on P3. *Biological Psychology*, *73*, 298–313.
Yago, E., Escera, C., Alho, K., Giard, M., & Serra-Grabulosa, J. M. (2003). Spatiotemporal dynamics of the auditory novelty-P3 event-related brain potential. *Cognitive Brain Research*, *16*, 383–390.
Yao, D. (2002). The theoretical relation of scalp Laplacian and scalp current density of a spherical shell head model. *Physics in Medicine and Biology*, *47*, 2179–2185.

(Received October 7, 2008; Accepted March 5, 2009)

Supporting Information

Additional Supporting Information may be found in the online version of this article:

Animated ERP and CSD topographies may be viewed at: http://psychophysiology.cpmc.columbia.edu/novelty2008.htm

Appendix S1. CSD-PCA of early vs. late blocks.

Figure S1. Reproducibility of solution and group differences across blocks.

Appendix S2. Hemispatial PCA.

Figure S2. Hemispatial PCA.

Please note: Wiley-Blackwell are not responsible for the content or functionality of any supporting materials supplied by the authors. Any queries (other than missing material) should be directed to the corresponding author for the article.

Accepted for publication in *Psychophysiology* ©2009 Society for Psychophysiological Research

Supplementary Material

Reproducibility of early novelty source

CSD-PCA of early vs. late novels. Novelty P3 has been reported to shift in topography with stimulus repetition (Friedman & Simpson, 1994), and an ICA study has noted some evidence of habituation (Debener et al., 2005). Inasmuch as each of the unique stimuli in the class of novels is presented only once, it could be argued that the results differentially reflect contributions by early (or late) trials in the trial sequence. An additional PCA was conducted based on correct novels which were separately averaged for blocks in first and last halves of the task (four conditions: first novel, last novel, nontarget, target). The subsequent PCA extracted essentially the same factors, factor score topographies, and group differences (Fig. S1).

A repeated measures ANOVA for the early central novelty source (*241*), using an additional within-subjects factor of sequence (first half, last half), replicated the overall difference between groups ($F[1,89] = 8.49$, $p = .005$; with age covariate: $F[1,88] = 4.35$, $p = .04$), but showed no evidence of a difference between first and last halves (sequence main effect and group x sequence interaction, both $F[1,89] < 1.0$, both n.s.). In contrast, the later frontal novelty source (*343*) showed prominent sequence effects (sequence main effect, $F[1,89] = 7.84$, $p = .006$; group x sequence interaction, $F[1,89] = 3.65$, $p = .06$), but did not differ between groups.

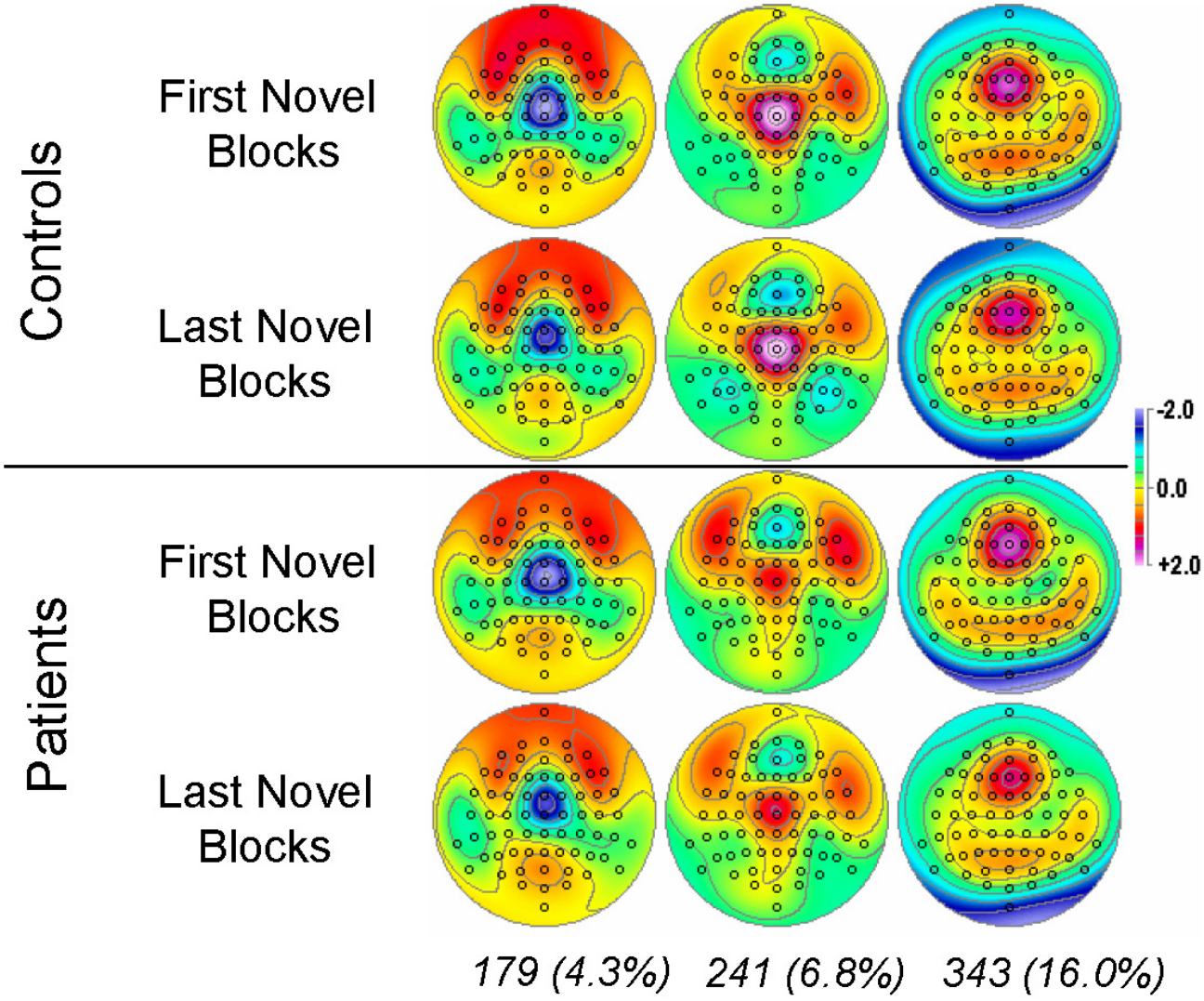

Figure S1. Factor score topographies of factors *179*, *241* and *343* for control and patient novelty response during first and last halves of task. A four-condition CSD-PCA (first novel, last novel, nontarget, target) extracted essentially identical factors, with comparable factor score topographies and group differences for each half. Scale: blue sink, red source.

Hemispatial PCA

To the extent that an ERP component may be identified with a specific neuroanatomical generator, it could be argued that the fundamental, and most stable property of a component is its topography. Since a spatial stability does not necessarily imply a corresponding temporal stability, it is possible that temporal PCA misrepresents the underlying component structure by inadequately or inappropriately misallocating the spatial variance over time. This possibility can be discounted if a spatial PCA results in a compatible solution, particularly for the critical, novelty vertex source. Conversely, spatial analyses must only be viewed as being confirmatory, since spatial CSD-PCA solutions tend to mirror the localization produced by CSD by producing components (regions) that are identifiable as individual electrodes (Tenke & Kayser, 2008).

To this end, a hemispatial PCA (Tenke et al., 2008) was conducted, in which each complete topography was reduced to a pair of hemispheric topographies consisting of the 28 homologous lateral sites and the 11 midline sites (i.e., midline data repeated to map each hemisphere to the midline). Hemitopographies were then submitted to a spatial PCA using a covariance matrix (39 variables = sites/hemisphere; 181,104 observations = 588 waveforms [2 hemispheres x 3 conditions x 98 participants x 308 time points]) followed by unrestricted Varimax rotation. Hemispatial solutions were then compared with the usual temporal solutions, with an emphasis on factors unique to the novelty oddball task.

As shown in Fig. S1, the hemispatial CSD-PCA solution identified focal regions comparable to those identified by factor score topographies in the temporal solution. Factor score waveforms closely resembled the averaged waveforms shown in Fig. 4. Notably, the novelty source had shorter latency for *Cz* than *Fz,* and was larger for controls than patients at *Cz*, but not at *Fz*.

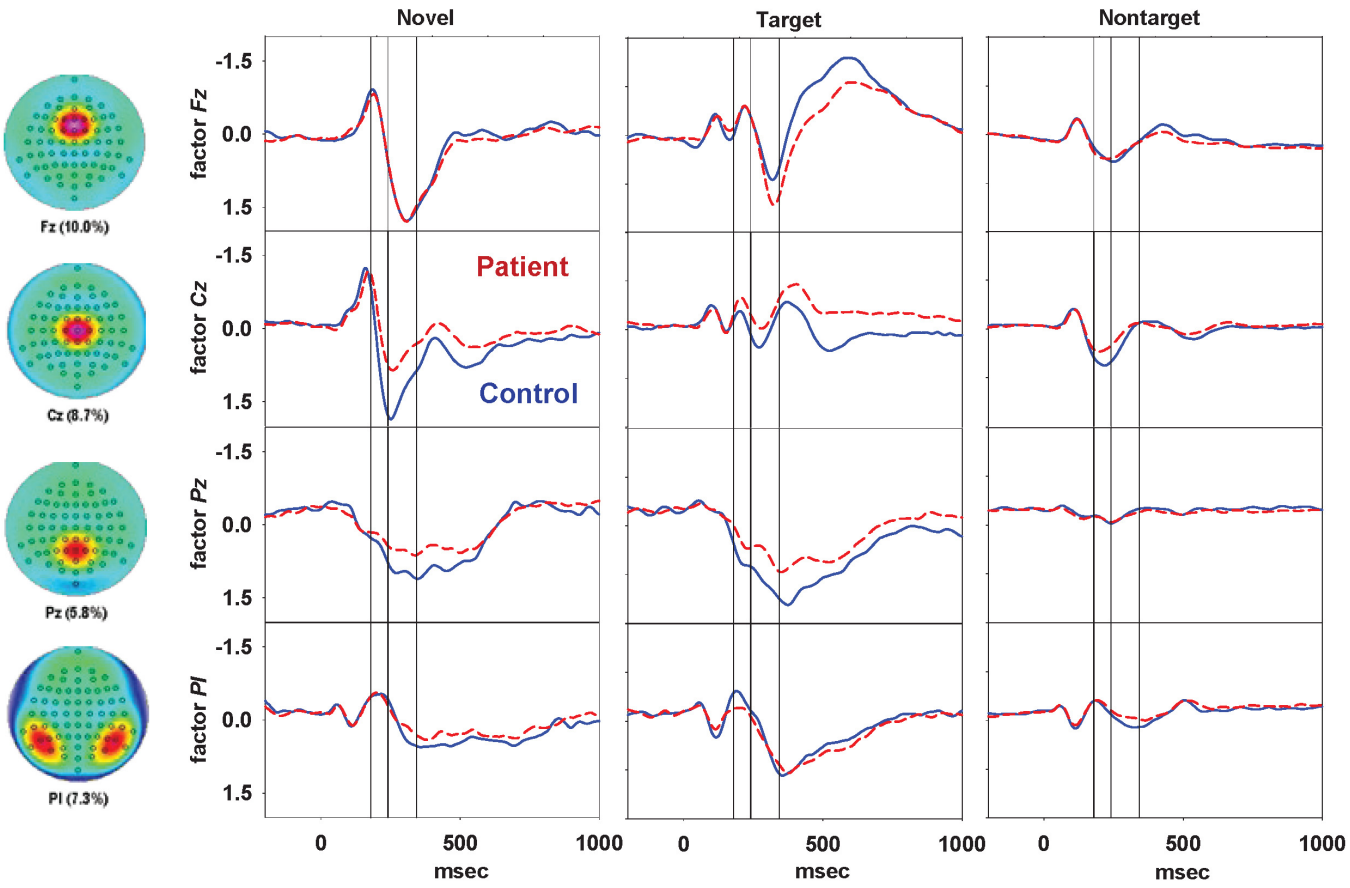

Figure S2. Left. First four hemispatial factor loadings topographies (percent variance in parentheses), identifiable as frontal (Fz), central (Cz) and parietal (Pz) midline, and parietal lateral (Pl) regions, respectively. Right. The corresponding average factor score waveforms are shown for each condition (controls: solid lines; patients: dashed lines. vertical lines at 179, 241 and 343 ms). Scale: negative-up (sink).